Journal of Data Acquisition and Processing
ISSN: 1004-9037
https://sjcjycl.cn/
DOI: 10.5281/zenodo.776851

UNSTEADY MHD DISSIPATIVE SQUEEZING FLOW OF CASSON FLUID OVER HORIZONTAL CHANNEL IN THE PRESENCE OF RADIATION AND CHEMICAL REACTION

***[1]G. Neeraja, [2]A. Saila Kumari**
[1]Research Scholar, Department of mathematics, JNTUA College of Engineering, Anantapur-515002, Andhra Pradesh, India. Email: pranav.hasini@gmail.com
[2]Assistant Professor, Department of mathematics, JNTUA College of Engineering, Anantapur-515002, Andhra Pradesh, India. Email: asailakumari@gmail.com

ABSTRACT:

In the field of computational fluid dynamics, one of the most well-known research issues is the interaction between the flow of liquid and chemical reactions. According to the findings of a significant number of studies, it has a variety of applications in industry, one of which is the modeling of flow inside nuclear reactors, and many researchers have lauded it for this. Motivated by the use of flow in industrial challenges, this study analyses the impacts of chemical reaction on the magnetohydrodynamic (MHD) squeezing Casson fluid flow through a porous medium under the slip condition with viscous dissipation the presence of radiation parameter. The flow is produced when two plates are compressed together in close proximity to one another. Using similarity variables may successfully convert partial differential equations (PDEs) to ordinary differential equations (ODEs). The shooting technique was used to perform the numerical analysis, which entailed solving the competent governing equations with dominating parameters for a thin liquid layer. This was done to determine the results of the study. It is essential to evaluate the numerical results in light of previously conducted research to validate the current answers. According to the results, an increase in the distance between the two plates leads to a rise in the velocity and the wall shear stress. The gas's velocity, temperature, and concentration all drop due to an increase in the Hartmann and Casson parameters. Both the temperature and the rate of heat transfer rise in direct proportion to the amount of viscous dissipation. In addition, it has been shown that the rate of mass transfer rises during destructive chemical interactions, but during constructive chemical reactions, the contrary occurs, which results in adverse effects.

Key words: Chemical reaction, Radiation parameter, Squeezing flow; viscous dissipation; Slip boundary

Introduction:

In the manufacture of hydrodynamical machines, accelerators, compression, injection molding, lubrication equipment, and polymer processing, amongst other processes, the unsteady squeezing channel flow, which is caused by the moving boundary under the influence of external everyday stresses or vertical velocities, is frequently encountered. The moving edge causes this flow because of the impact of steep rates or everyday external pressures. Since Stefan [1] began the study of squeezing flow using the lubrication approximation, numerous scholars have sequentially investigated squeezing flow issues for various geometrical configurations using a wide variety of approaches. Moore [2] concluded that the Stefan equation is insufficient to describe the molecular mechanism of viscosity of squeezing flows. Instead, he indicated that the influences such as surface finish, viscoelastic liquids, elastomeric surfaces, and molecular effects also need to be considered partially or entirely depending on the complexity of the problems. Gupta et al. [3] noticed that the unsteady squeezing channel flow problem could be significantly simplified via similarity variables. The distance between the paralleled plates varies as the square root of a linear function of time. In this scenario, the similarity variables allow the problem to be significantly simplified. Duwairi et al. [4] studied heat transfer effects on unsteady squeezing channel flow, and they assumed that the paralleled walls were heated evenly at a constant temperature. This allowed them to examine the impact of heat transfer on the flow. Different scholars, such as Verma [5], Mustafa et al. [6], and Hayat et al. [7], conducted more studies into the unstable squeezing flow difficulties by taking into account a variety of physical challenges and computational methodologies.

Squeezing flow between parallel plates is an important problem in the area of fluid dynamics. The problem can be described akin to the principle of moving pistons, where the squeezing behavior of two parallel plates produces a flow that is normal to the plates. Applications of the problem are found in hydraulic machinery and tools, electric motors, food industry, bioengineering, and automobile engines. Other simpler but equally important examples are flow patterns occurring in syringes and compressible tubes. In these applications, flow patterns can be classified into laminar, turbulent, and transitional flows on the basis of the well-known Reynold’s number. From an industrial perspective, it is necessary to study the effect of these different behaviors for non-Newtonian fluids, the mechanics of which have proved to be a significant challenge to the research community. The non-Newtonian fluid model being considered in our case is that of Casson [8, 9] as it is able to capture complex rheological properties of a fluid, unlike other simplified models like the powerlaw [10] and grade-two or grade-three [11] models. Concentrated fluids like sauces, honey, juices, blood, and printing inks [12] can be well described using this model. More formally, Casson fluid can be defined as a shear thinning liquid which is assumed to have an infinite viscosity at zero rate of shear, a yield stress below which no flow occurs, and a zero viscosity at an infinite rate of shear [13]. Application of Casson fluid for flow between two rotating cylinders is performed in [14]. In some industrial applications, the model has to deal with conducting fluids which exhibit different behaviors under the influence of a magnetic field. In these cases, the magnetohydrodynamic (MHD) aspect of the flow needs to be considered. In this article, we investigate this particular case for a porous medium channel and present a comprehensive analysis. To the best of our knowledge, this particular case has not been addressed before. A porous medium, identified as a material that contains fluid-filled pores, is always characterized by properties such as porosity and permeability. Porosity defines the quantity of fluid that can be held by the material, whereas permeability is the amount of fluid that can pass through it. Various applications include ground water hydrology, chemical reactors, irrigation, drainage, seepage, and recovery of crude oil from pores of reservoir rocks [15–19]. These applications can specifically be classified to engineering fields such as petroleum, reservoir, and chemical engineering.

The study of heat and mass transport in combination with chemical reactions is of significant practical value to engineers and scientists because it occurs practically everywhere in various engineering and scientific disciplines. This makes it an area of study that has a substantial amount of application potential. This kind of flow has the potential to be used in a wide variety of industries, including, to mention just two examples, the chemical process industry, and the power industry. The impacts of diffusion thermal, radiation absorption and chemical reaction on the MHD free convective heat and mass transfer flow of a nanofluid confined within a semi-infinite flat plate were examined by Prasad et al. [20]. An unstable Casson nanofluid flow was used by Samrat et al. [21] in their study on the influence of heat radiation on the flow. This flow was conducted on a stretched surface. The effects of chemical reactions on different flow geometries have been studied by Raghunath and colleagues [22–24] under the impact of thermal diffusion, chemical reaction, and a heat source. The effects of Soret on the unsteady free convection flow of a viscous incompressible fluid through a porous medium with high porosity confined by a vertical infinite moving plate with high porosity were examined by Ramachandra et al. [25]. The influence of frictional heating on the mixed convection flow of a chemically reacting Casson nanofluid over an inclined porous plate was studied by Sulochana et al. [26]. The researchers looked at the flow of the nanofluid across the plate. The effect of radiation absorption on an unsteady convective heat and mass transfer flow through a semi-infinite inclined permeable plate was investigated by Rani and Murthy [27] using a semi-infinite inclined permeable plate that was submerged in a porous medium.

The current effort is primarily concerned with the simulation of flow in a nuclear reactor. For the purpose of investigating the flow of nuclear reactions in a nuclear reactor, it is necessary to include chemical reaction in the mathematical model as a component. It has been revealed that the inability to manage nuclear reactions may result in extensive pollution of the environment, including air and water. As a result, when a nuclear power plant disaster occurs, the nuclear reaction flow is halted instantly [28]. Furthermore, the relevance of MHD and porous media in the fluid flow is discussed in detail. In their study, Song et al. [29] discovered that MHD had the best efficiency of the numerous power conversion systems tested. The efficiency of the power conversion is critical to the NEP system. Essentially, nuclear electric propulsion (NEP) is a kind of electric propulsion in which a nuclear reactor generates power. Saadati et al. [30] stated that a porous medium method was used to increase the safety margin of a nuclear reactor. One of the most pressing challenges in the operation of nuclear power plants is the need to enhance the amount of heat removed from the reactor. In this way, porous media in nuclear reactors increases the rate of heat evacuation from the reactor. Shankar et al. [31] have studied Magnetized impacts of Brownian motion and thermophoresis on unsteady squeezing flow of nanofluid between two parallel plates with chemical reaction and Joule heating. Recently Noor et al. [32] have possessed Unsteady MHD Squeezing Flow of Casson Fluid over Horizontal Channel in Presence of Chemical Reaction.

Thermal radiation is more significant in high-temperature environments, which may be found in many engineering domains, particularly for small convective thermal transfer. This is notably the case for small convective thermal transfer. In addition to this, such radiation plays an essential part in managing the thermal transfer scheme and the thermally maintained procedure used in the polymer manufacturing business. In light of this fact, the researchers have begun their investigation into the effects of radiation on fluid flow systems. For example, Mandal and Mukhopadhyay [33] used a shooting scheme to reveal their findings on the thermal research of a micropolar liquid moving past a stretched surface while considering the effect of radiated environmental factors. With the assistance of the shooting technique and the Runge-Kutta method, Kumar et al. [34] were able to successfully simulate the motion of Casson liquid as it moved past a stretched curved surface while being affected by heat radiation.

Along with natural convection, the thermal radiation features of the electrically conducting nanofluid were investigated by Ghadikolaei et al. [35]. In addition to this, the research on the flow of non-Newtonian liquids via porous space has obtained a spectacular consideration with the logic that such transport considerably contributes to sedimentation, space pollution, blood movement arteries, and loaded beds. Asghar and colleagues [36] have presented a theoretical inquiry on the physiological fluid flow in a curved channel while considering the impacts of a porous material. Ramesh [37] proposed an investigation that coupled the stress of a liquid stream with a pumping method while considering the effect of MHD and a porous medium. The motion of cilia was studied by Akbar et al. [38], who used the pumping and propulsion of a viscous liquid inside a horizontal tube containing a porous media. The analytical solutions for the propulsion of MHD Ree-Eyring liquid between the plates in different conditions concerning the motion of the plates under various influences have been presented by Ramesh and Eytoo [39]. Under the effects of magnetohydrodynamics, Joule heating, and electro-osmosis, Ramesh et al. [40] have explored the motion of pair stress fluids in the porous channel. The MHD squeezing flow of Casson nanofluid with chemical reaction, thermal radiation, and heat generation/absorption has been reviewed by Noor et al. [46]. Naduvinamani and Usha Shankar [47] investigated the radiative squeezing flow of unstable magneto-hydrodynamic conditions. Casson fluid in between two plates that is parallel to one another.

According to the papers detailed earlier, it has not yet been established whether or not chemical reactions affect the squeezing flow of Casson fluid across a porous medium with viscous dissipation. In addition to this, it has been seen that the sliding boundary condition is not given as much consideration as it should be. Consequently, the study is concentrated on time-dependent MHD squeezing slip flow of Casson fluid through porous media with chemical reaction and joule dissipation in the presence of radiation parameters. The numerical solutions may be obtained with the use of the shooting method. In addition, the correctness of the current outputs has been checked by comparing them to the results that have been published in peer-reviewed papers. In this study, we investigate the impact that key parameters have on the fluid's concentration, temperature, and velocity.

1. Non-Newtonian Casson fluid model

To create the governing equations for Casson fluid flow when it is compressed between two parallel plates, the rheological equation [41] shown below is employed.

$$\tau_{ij} = \begin{cases} 2\left(\mu_B + \dfrac{P_y}{\sqrt{2\pi}}\right) e_{ij}, \pi > \pi_{c,} \\ \left(\mu_B + \dfrac{P_y}{\sqrt{2\pi_C}}\right) e_{ij}, \pi < \pi_{c,} \end{cases}$$

(1)

In equation (7), $\pi = e_{ij}, e_{ij}$, Where e_{ij} are the $(i, j)\, th$ Component of the deformation rate, π is the product of the deformation rate with itself, π_C is a critical value of this product based on the non-Newtonian model, μ_B is the plastic dynamic viscosity of the non-Newtonian fluid and P_y the yield stress of the fluid.

$$P_y = \frac{\mu_B \sqrt{2\pi}}{\beta} \tag{2}$$

Denote the yield stress of fluid. Some fluids require a gradually increasing shear stress to maintain a constant strain rate and are called Rheopectic, in the case of Casson fluid (Non-Newtonian) flow where $\pi > \pi_c$

$$\mu = \mu_B + \frac{p_y}{\sqrt{2\pi}} \tag{3}$$

When Equation (2) is substituted into Equation (3), the kinematic viscosity may be expressed as

$$\vartheta = \frac{\mu}{\rho} = \frac{\mu_B}{\rho}\left(1 + \frac{1}{\beta}\right)$$

(4)

Where $\beta = \dfrac{\mu_B \sqrt{2\pi_c}}{p_y}$ denotes the Casson fluid parameter. The nature of Non-Newtonian fluid vanishes and it behaves as Newtonian fluid when $\beta \rightarrow \infty$.

2. Formulation of the Problem

The time dependent MHD flow of Casson fluid through porous medium with chemical reaction, joule dissipation and velocity slip are explored. The squeezing of two surfaces generates the flow in the channel. The distance of two surfaces is $y = \pm h\,(t) = \pm(1 - \alpha t)^{1/2}$. The two surfaces are moving further as $\alpha < 0$ and the surfaces are moving closer as $\alpha > 0$ till $t = 1/\alpha$ with velocity $v_w(t) = \partial h(t)/\partial t$. The lower plate is exerted with the magnetic field (t)

vertically [32]. Figure 1 portrays the geometrical model of Casson fluid flow. Also, the homogeneous first order chemical reaction effect is accounted in the concentration equation. Further, in the present analysis, symmetric flow is assumed. With these assumptions, the continuity, momentum, energy and concentration equations governing the present physical problem with necessary conditions are as follows [46, 47].

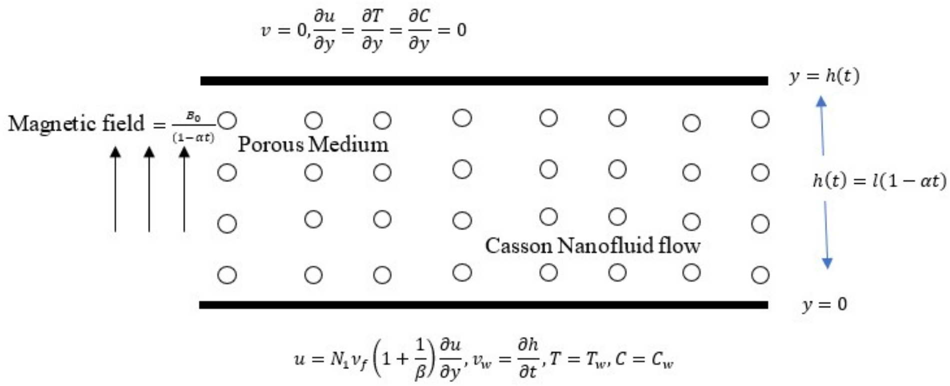

FIGURE: 1 Physical model of problem

$$\frac{\partial u}{\partial x}+\frac{\partial u}{\partial y}=0$$

(5)

$$\frac{\partial u}{\partial t}+u\frac{\partial u}{\partial x}v\frac{\partial u}{\partial y}=v_f\left(1+\frac{1}{\beta}\right)\frac{\partial^2 u}{\partial y^2}-\frac{\sigma B^2(t)}{\rho_f}u-v_f\left(1+\frac{1}{\beta}\right)\frac{\varphi}{k_1(t)}u \tag{6}$$

$$\frac{\partial v}{\partial t}+u\frac{\partial v}{\partial x}v\frac{\partial v}{\partial y}=v_f\left(1+\frac{1}{\beta}\right)\frac{\partial^2 v}{\partial y^2}-\frac{\sigma B^2(t)}{\rho_f}v-v_f\left(1+\frac{1}{\beta}\right)\frac{\varphi}{k_1(t)}v \tag{7}$$

$$\frac{\partial T}{\partial t}+u\frac{\partial T}{\partial x}v\frac{\partial T}{\partial y}=\alpha_f\frac{\partial^2 T}{\partial y^2}+\frac{v_f}{c_f}\left(1+\frac{1}{\beta}\right)\left[4\left(\frac{\partial u}{\partial x}\right)^2+\left(\frac{\partial u}{\partial y}\right)^2\right]-\frac{1}{\rho_f c_f}\frac{\partial q_r}{\partial y}+\frac{1}{\rho_f c_f}\frac{Q(t)}{T}$$

(8)

$$\frac{\partial C}{\partial t}+u\frac{\partial C}{\partial x}v\frac{\partial C}{\partial y}=D_m\frac{\partial^2 C}{\partial y^2}-k_c(t)C$$

(9)

Where, $\alpha_f=\frac{k}{(\rho c)_f}$ is the thermal diffusion of Casson fluid, $k_c(t)=k_2(1-\alpha t)^{-1}$ is the rate of chemical reaction and $k_1(t)=k_0(1-\alpha t)$ is the permeability of porous medium.

The correlated boundary conditions (BCs) are

$$u=N_1 v_f\left(1+\frac{1}{\beta}\right)\frac{\partial u}{\partial y},\ v=vw=\frac{\partial h(t)}{\partial t}\text{, at } y=h(t), \tag{10}$$

$$\frac{\partial u}{\partial y}=0,\quad v=0,\quad \frac{\partial T}{\partial y}=0,\quad \frac{\partial C}{\partial y}=0,\qquad \text{at } y=0 \tag{11}$$

Where $N_1(t) = N_0(1-\alpha t)^{1/2}$ represent momentum slip.

For an optically thick fluid, in addition to emission there is also self absorption and usually the absorption co-efficient is wavelength dependent and large so we can adopt the Rosseland approximation for the radiative heat flux vector qr. Thus qr is given by

$$q_r = \frac{-4\sigma_1}{3k_1}\frac{\partial^2 T^4}{\partial z^2}$$

(12)

Where k_1 is Rosseland mean absorption co-efficient and σ1 is Stefan–Boltzmann constant.

We assume that the temperature differences within the flow are sufficiently small so that T^4 can be expressed as a linear function. By using Taylor's series, we expand T′4 about the free stream temperature T_∞ and neglecting higher order terms. This results in the following approximation:

$$T^4 \approx 4T_\infty^3 T^* - 3T_\infty^4$$

(13)

THE ENERGY EQUATION IS DERIVED USING EQUATIONS (12) AND (13) AS FOLLOWS

$$\frac{\partial T}{\partial t} + u\frac{\partial T}{\partial x} v\frac{\partial T}{\partial y} = \alpha_f \frac{\partial^2 T}{\partial y^2} + \alpha_f\left(\frac{16\sigma T_\infty^3}{3k_f k_1^*}\right)\frac{\partial^2 T}{\partial y^2} + \frac{v_f}{c_f}\left(1+\frac{1}{\beta}\right)\left[4\left(\frac{\partial u}{\partial x}\right)^2 + \left(\frac{\partial u}{\partial y}\right)^2\right] + \frac{1}{\rho_f c_f}\frac{Q(t)}{T} \tag{14}$$

The similarity transformation used in Pourmehran et al., [45] and Noor et al., [46] is imposed to transform the PDEs to dimensionless ODEs

$$\eta = \frac{y}{l\sqrt{(1-\alpha t)}},\quad u = \frac{ax}{2(1-\alpha t)} f'(\eta),\quad v = \frac{al}{2\sqrt{(1-\alpha t)}} f(\eta),\quad \theta = \frac{T}{T_w},\quad \phi = \frac{C}{C_w} \tag{15}$$

Substitute Eq. (15) into Eq. (6-9) yields to obtain the subsequent non dimensional equations

$$\left(1+\frac{1}{\beta}\right) f^{iv} - S(\eta f''' + 3f'' + ff'' - ff''') - Ha^2 f'' - \left(1+\frac{1}{\beta}\right)\frac{1}{Da} f'' = 0 \tag{16}$$

$$\frac{1}{\Pr}\left(1+\frac{4}{3}R_d\right)\theta'' + S(f\theta' - \eta\theta' + Q\theta) + E_c\left[\left(1+\frac{1}{\beta}\right)(f'')^2 + 4\sigma^2 (f')^2\right] = 0 \tag{17}$$

$$\frac{1}{Sc}\phi'' + S(f\phi' - \eta\phi') - R\phi = 0$$

(18)

The correlated Dimensionless boundary conditions (BCs) are

$$f(\eta)=0,\ f''(\eta)=0,\ \theta'(\eta)=0,\ \phi'(\eta)=0 \text{ at } \eta=0 \tag{19}$$

$$f(\eta)=1,\ f'(\eta)=\gamma\left(1+\frac{1}{\beta}\right)f''(\eta),\ \theta(\eta)=1,\ \phi(\eta)=1 \text{ at } \eta=1 \tag{20}$$

The significant parameters in the non dimensional equations are defines as

$$S=\frac{\alpha l^2}{2v_f},\ Ha=lB_0\sqrt{\frac{\alpha}{\rho_f v_f}},\ Da=\frac{k_0}{\phi l^2},\ \gamma=\frac{N_0 v_f}{l},\ \delta=\frac{1}{x}(1-\alpha t)^{1/2},\ \Pr=\frac{v_f}{\alpha_f},\ Sc=\frac{v_f}{D_m}$$

$$R=\frac{k_2 l^2}{v_f},\ Ec=\frac{\alpha^2 x^2}{4c_f T_w(1-\alpha t)^2},\ R_d=\frac{4\sigma T_\infty^3}{k_f k_1^*},\ \gamma=\frac{2Q_0}{\alpha(\rho c)_f}$$

Physically, the movement of channel is portrayed by squeezing number with $S>0$ shows the plates approaches closer and $S<0$ shows the plates separates further. Darcy and Hartmann numbers are important parameter for velocity profile. Furthermore, thermal radiation, Eckert number and heat generation/absorption parameters are used for regulation of temperature profile. The effect of chemical reaction is exhibited in the nanoparticles concentration profile. The flow in the simultaneous momentum and mass diffusion is described by Schmidt number.

Physical quantities of Interests

The physical quantities of interest which govern the flow are the local skin friction coefficient C_{fx}, local Nusselt number N ux and local Sherwood number S hx, which are defined as

$$Cf_x=\frac{\tau_w}{\rho f u_w^2},\ Nu_x=\frac{xq_w}{\alpha_f\left(T_w-T_\infty\right)},Sh_x=\frac{xq_s}{D_B\left(C_s-C_\infty\right)}$$

where τw, qw and qs are the wall skin friction, wall heat flux and wall mass flux respectively given by

$$\tau_w=\mu_B\left(1+\frac{1}{\beta}\right)\left[\frac{\partial u}{\partial y}\right]_{y=h(t)},\qquad q_w=-\alpha_f\left[\frac{\partial T}{\partial y}\right]_{y=h(t)},\qquad q_s=D_m\left[\frac{\partial C}{\partial y}\right]_{y=h(t)}$$

The non-dimensional forms of the skin friction coefficient, Nusselt number and Sherwood number in terms of similarity variable are

$$\frac{l^2}{x^2}(1-at)\mathrm{Re}_x\,Cf_x=\left(1+\frac{1}{\beta}\right)f''(1),$$

$$\sqrt{(1-at)}\,Nu_x=-\theta'(1),$$

$$\sqrt{(1-at)}\,Sh_x=-\phi'(1),$$

3. RESULTS AND DISCUSSION:

The ordinary differential equations (16)– (18) With conditions (19-20), governing the radiative squeezing flow of unsteady magneto-hydrodynamic Casson fluid between two parallel plates are coupled and nonlinear in nature. Hence, to solve these complex flow equations, numerically stable Runge-Kutta fourth order integration algorithm with standard shooting technique [48] is used. To confirm the accuracy of the present numerical scheme and correctness of the obtained numerical solutions, the results are compared with those of Noor et al [46] and Naduvinamani, Usha Shankar [47]. This comparison is shown in Table 1. From Table 1 it is observed that, the present numerical results are exactly matching with the semi-analytical results of Ref. [46,47]. Also, it is noticed from Table 1 that, the absolute values of wall shear stress are enhanced for the increasing values of squeezing number, whereas, the Nusselt and Sherwood numbers decrease. Also, it is obvious that, the negative values of the

Nusselt number indicate the flow of heat from the surface of parallel plates to the fluid between the plates.

TABLE 1

COMPARISON OF $-f''(1)$, $-\theta'(1)$ AND $-\phi'(1)$ FOR DIFFERENT VALUES OF S WHEN $\beta \rightarrow \infty$, $Da \rightarrow \infty$ AND $Ha = Rd = \gamma = Nb = Nt = 0$

S	NOOR ET AL [46]			NADUVINAMANI AND USHASHANKA [47]			PRESENT VALUES		
	$-f''(1)$	$-\theta'(1)$	$-\phi'(1)$	$-f''(1)$	$-\theta'(1)$	$-\phi'(1)$	$-f''(1)$	$-\theta'(1)$	$-\phi'(1)$
-1.0	2.170255	3.319904	0.804558	2.170091	3.319899	0.804559	2.170851	3.317499	0.808545
-0.5	2.617512	3.129556	0.781404	2.617404	3.129491	0.781402	2.617547	3.124588	0.787585
0.01	3.007208	3.047166	0.761229	3.007134	3.047092	0.761225	3.006774	3.047758	0.767582
0.5	3.336504	3.026389	0.744229	3.336449	3.026352	0.744224	3.334578	3.024785	0.744785
2.0	4.167412	3.118564	0.701819	4.167389	3.118551	0.701813	4.164755	3.118568	0.701714

To describe the physical insight of the present problem in depth, the thermodynamic flow behaviour of skin-friction coefficient, Nusselt and Sherwood numbers along with velocity, temperature and concentration profiles in the flow region for different set physical parameters namely, squeezing parameter (S), Casson fluid parameter (β), Hartmann number (Ha), radiation parameter (R), heat generation or absorption parameter (Q), Eckert number (Ec), Prandtl number (Pr), chemical reaction parameter (Kr) and Schmidt number (Sc) are investigated. For better understanding of the numerical results, the computer generated numerical data are presented in the form of graphs and tables.

Effect of squeezing number

The thermodynamic behaviour of velocity, temperature and concentration profiles for different values of squeezing number (S) is depicted in Figures 2–7 with fixed values of β=0.8, Ha=R=Q=Ec=Kr=0.1, Pr=0.1 and Sc=0.7. The movement of the parallel plates moving away from one another (S>0) is illustrated by Figures 2, 3 and 4. Similarly, the movement of the parallel plates coming close to one another (S<0) is described by Figures 5, 6 and 7 in the flow region. For positive values of squeezing number, radial velocity field (F) decreases from η=0 to η=1 and radial velocity profile increases from η=0 to η=1 for negative values of S. These changes in radial velocity fields are clearly shown in Figures 2 and 5, respectively. This increment in velocity field is due to the reason that, when parallel plates move apart from one another, fluid is sucked into the channel consequently which increases the velocity field. In other case, when plates move close to one another, liquid inside the channel is emitted out which gives the liquid dropping inside the channel and hence velocity of the fluid decreases. However, squeezing number is a function of velocity field in the flow region.

Figures 3 and 6 show the thermodynamic differences seen in the temperature profile (θ) for both S > 0 and S0 in the flow zone. These variations were observed in the temperature profile. Figure 2 illustrates how the temperature field is finally suppressed for the cases in which the squeezing number is allowed to increase in a positive direction. This drop in the temperature field is because a higher value of the squeezing number reduces the squeezing force exerted on the flow, which in turn has a negative impact on the temperature field. On the other hand, looking at Figure 6, one can see an increase in the magnitude of the temperature field for S = 0. Since the magnifying value of the squeezing number is closely related to the decaying of the kinematic viscosity, the distance between parallel plates, and the speed at which plates move, it is evident that the temperature field is relatively high when plates move close to one another. This is the case because of the close relationship between these three factors. On the other hand, the temperature profile exhibits the behavior of a function that steadily increases from zero to one. This much is abundantly apparent. Nevertheless, the impact of S on the concentration profile in the flow zone is seen in figures 4 and 7. An increased concentration field may be seen for S values greater than zero, as seen in figure 4. Furthermore, looking at Figure 7, one can see that the concentration field goes down when S is made smaller than 0. In addition, Figure 7 reveals that the influence of the compressing number decreases with greater values. This is something that can be seen. Therefore, the concentration profile is a function of the number of times the substance was squeezed.

Influence of Casson fluid parameter

The impact of Casson fluid parameter on velocity, temperature and concentration profiles is described in Figures 8–10 with fixed S=Ha=0.5, R=Q=Kr=0.1, Sc=0.7, Pr=0.7 and Ec=0.8.

It can be seen in Figure 8 how the value affects the axial velocity profile. Figure 8 reveals that a rise in the value results in a greater axial velocity field below 0.5, but the opposite is seen in the channel section above 0.5. This can be seen by comparing the two regions. In addition, due to these shifts in the axial velocity field at the channel's edges, there is a tendency toward cross-flow in the channel's center area.

In addition, Figure 9 illustrates how the value describes how the value influences the temperature profile. Figure 9 indicates quite clearly that there is a negative correlation between an increase in the Casson fluid parameter and a drop in the temperature field in the flow zone. In addition, the thickness of the thermal boundary layer decreases when the Casson fluid parameter is increased to higher and higher values. However, the reduction in thickness of the thermal boundary layer is caused by an increase in the elasticity stress variable. A thinner thermal boundary layer is comparable to lower thermal diffusivity values, which demonstrates a higher temperature differential in the region of parallel plates. This is the case because similar plates have a reduced ability to dissipate heat. In addition to this, the temperature field is a function of that lower, and this decline occurs from =0 to =1.0. The temperature field may be normalized by raising the values. This is possible because it appears directly in the thermal equation (see Eq. (8)). In addition to this, it can be shown from Figure 10 that each of the curves in concentration profiles overlap with one another, which suggests that does not have a significant impact on concentration profiles. This is because it does not explicitly appear in the mass diffusion equation (refer to Eq. (14)).

Effect of Hartmann number (Ha)

The influence of Hartmann number on flow behaviour is described in Figures 11–13 with fixed values of Pr=0.7, Sc=0.7 and β=S=R=Q=Kr=Ec=0.1.

An increase in the Hartmann number results in a reduction in the standard component of the velocity profile in the flow zone, as can be seen in Figure 11. This is a self-explanatory illustration of the phenomenon. It is reasonable to anticipate that a negligible increase in the Hartmann number is to blame for the increased Lorentz forces associated with magnetic fields since this is pretty apparent. Because of the amplified Lorentz forces, the passage of fluid through the channel is met with an increasing amount of resistance. Consequently, it is to be anticipated that the velocity field will become less intense as the value of the Hartmann number rises. As a result, a tendency toward cross-flow may be seen at the channel's core part due to these differences in the axial velocity at the boundary. On the other hand, the temperature profile (θ) and the fluctuations seen in it for various Ha values are shown in Figure 12. It can be seen by looking at this figure that when the value of Ha goes greater, there is a muted effect on the temperature field. Because of an increase in the Hartmann number, there is a decrease in the elasticity stress variable. This decrease in elasticity stress variable is responsible for the deterioration of the thermal field in the flow region, which is responsible for observing a thinner temperature boundary layer. Additionally, the temperature field is a function of Ha that goes up as you increase it. In addition, it is incredibly essential to observe that, as shown in Figure 13, all of the concentration curves that regulate the concentration field are consistent. This is because Ha does not significantly influence the concentration profile. Ha does not appear explicitly in the concentration equation (see Eq. (11)).

Influence of radiation parameter (Rd)

The effect of radiation parameter on temperature profile is described in Figure 14 with fixed values of S=Ha=0.5, β=Q=Kr=0.1, Sc=0.7 and Ec=1.0, Pr=0.7. Figure 14 clearly portrays that, an upsurge in thermal radiation parameter eventually diminishes on the temperature profile in the flow region. This fact can be depicted through the relation $R_d = \dfrac{4\sigma T_\infty^3}{k_f k_1^*}$ Thus, in view of the relation $R_d = \dfrac{4\sigma T_\infty^3}{k_f k_1^*}$, a small upsurge in Rd causes the decay of absorption coefficient k_1^*, hence temperature profile decreases. Also, the slope of temperature curves close to the wall indicates that the heat flows from the surface plates to the fluid. Thus, from Figure 14 it is conclude that, the numerical results obtained in this figure are reasonable and are acceptable. Also, physically, an increment in thermal radiation parameter gives the greater temperature value which may be useful in many of the thermodynamic industries.

Impact of heat source/sink parameter (Q)

The influence of heat generation or absorption parameter (Q) on temperature profile is illustrated in Figures 15 with fixed values of S=Ha= 0.5, Pr=0.7, Sc=0.7 and β=R=kr=0.1, Ec=1.0. It is observed from Figure 15 that as Q increases, the temperature field increases. Also, the thickness of thermal boundary layer increases for increasing values of Q. It is expected that, during the heat generation process more temperature is usually released into the working fluid. Owing to this reason, the temperature profile upsurges as heat generation parameter increases. Also, due to the exothermic chemical reactions, the temperature field increases.

Effect of Prandtl number (Pr)

The influence of Pr on temperature profile is described in Figure 16 with fixed values of S=Ha=0.5, β=R=Q=Kr=0.1, Sc=0.7. It is observed from Figure 16 that, temperature field increases for increasing values of Pr. This increment in temperature profile is mainly due to decrease in the thermal conductivity values. However, dissipation effects are also responsible for the increase of temperature field in the flow. Further, the thickness of temperature boundary layer decreases [44] for increasing values of Pr. This decrement is mainly due to the fact that, the magnified Pr values greatly decrease the thermal diffusivity which in turn causes the decreasing of the temperature boundary layer thickness. Generally, it is known that, Pr1 corresponds to the high-viscosity materials like oils etc. From this observation it is concluded that, temperature field is an increasing function of Pr.

Influence of chemical reaction parameter (R)

The effect of chemical reaction parameter on concentration profile is illustrated in Figure 17. with fixed values of S=Ha=0.5, β=R=Q=Ec=0.1 and Pr=0.7, Sc=0.7. Generally, it is observed that, in many of the cases the decreased concentration field is noticed for destructive chemical reaction. In view of this, Figure 17 confirms the results obtained in Ref. [44]. Thus, Figure 17 clearly illustrates that, for the destructive chemical reaction concentration distribution decreases.

Effect of Schmidt number (Sc)

The influence of Schmidt number (Sc) on concentration profile with fixed values of S=Ha=0.5, β=R=Q=Ec=Kr=0.1 and Pr=0.7 is described in Figure 17. Figure 17 clearly illustrates that, the increasing Schmidt number decreases the concentration field in the flow region. This fact can be justified as follows: a small upsurge in Schmidt number diminishes the coefficient of mass diffusion, which in turn causes the decreases of concentration field in the flow region. Further, it is observed that, the concentration field is a decreasing function of Sc. Also, the concentration boundary layer thickness decreases for increasing values of Sc.

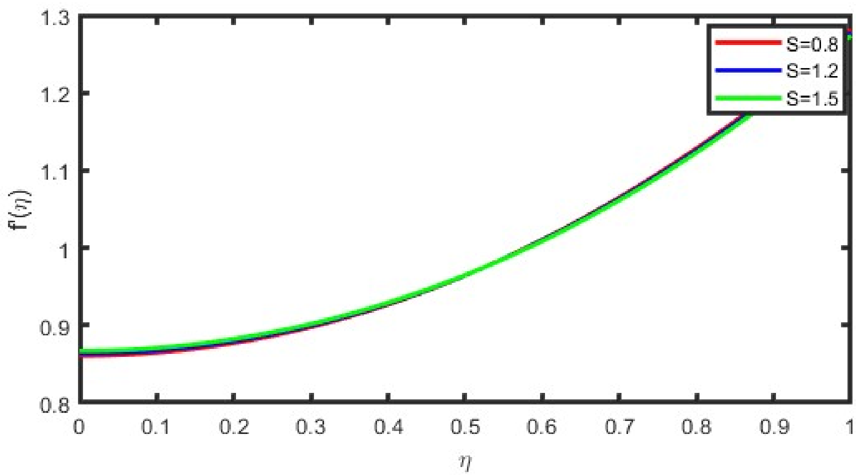

FIGURE 2 EFFECT OF S>0 ON F(H)

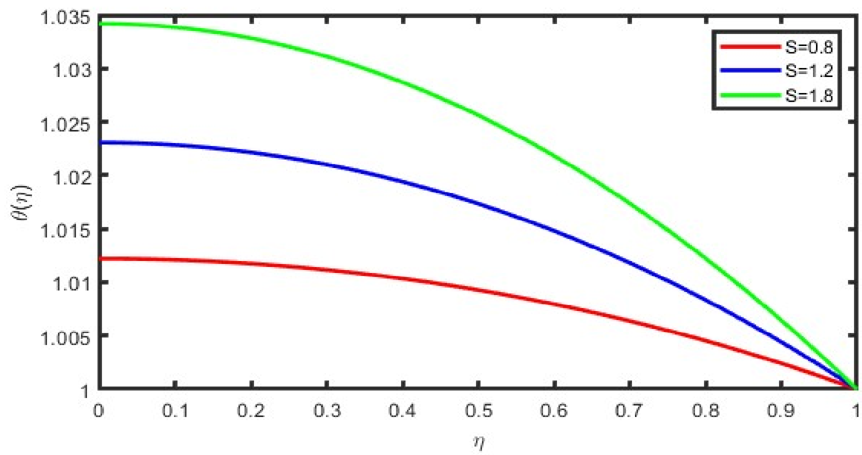

FIGURE 3 EFFECT OF S>0 ON Θ(H)

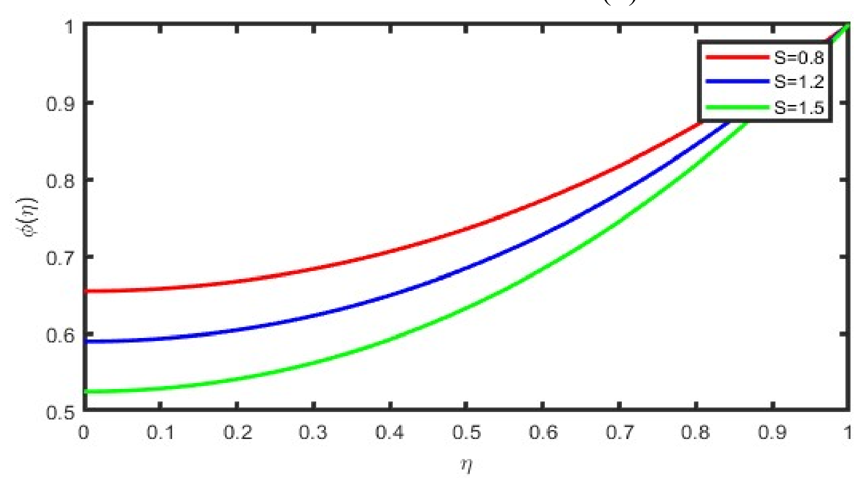

FIGURE 4 IMPACT OF S>0 ON ϕ (H)

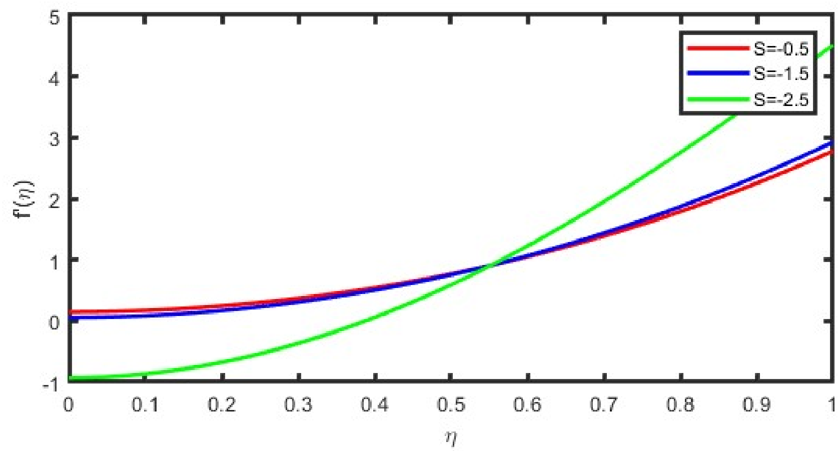

FIGURE 5 EFFECT OF S<0 ON F(H)

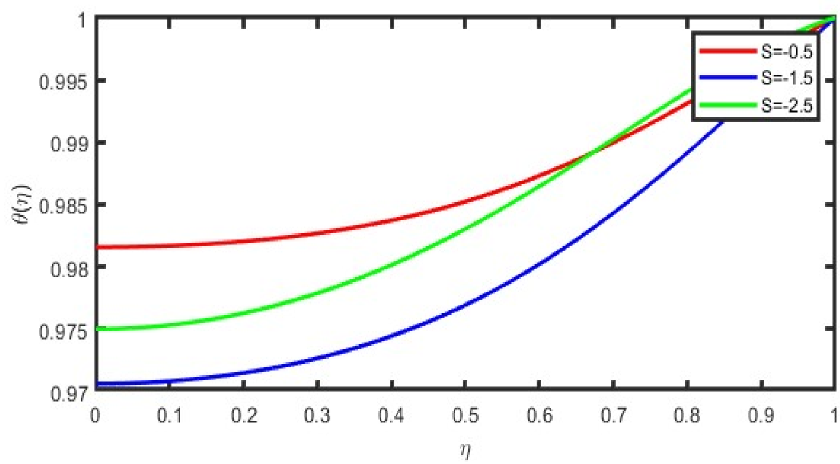

FIGURE 6 EFFECT OF S<0 ON Θ(H)

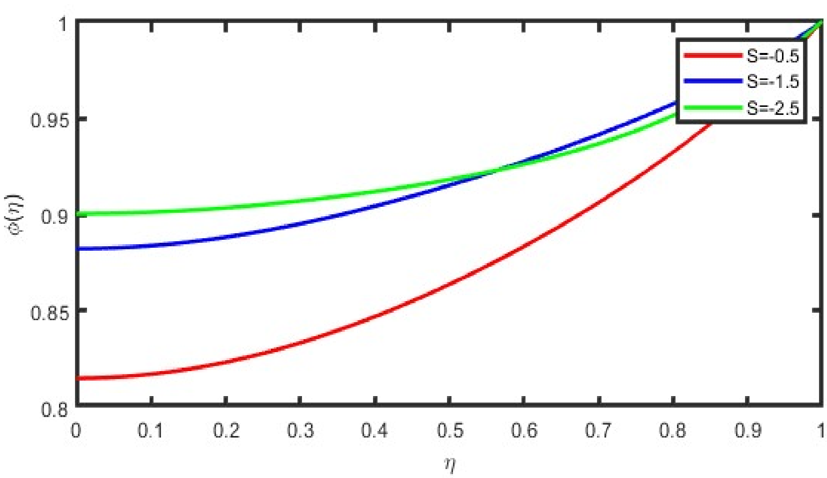

FIGURE 7 IMPACT OF S<0 ON ϕ (H)

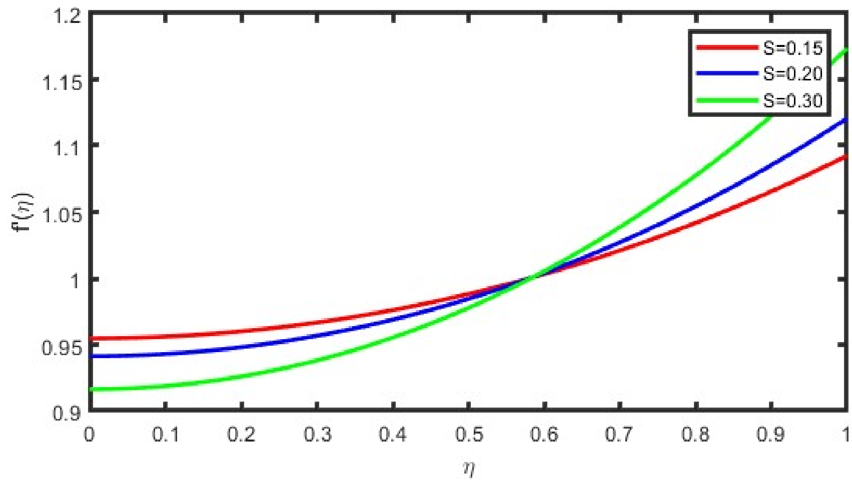

FIGURE 8 IMPACT OF B ON F(H)

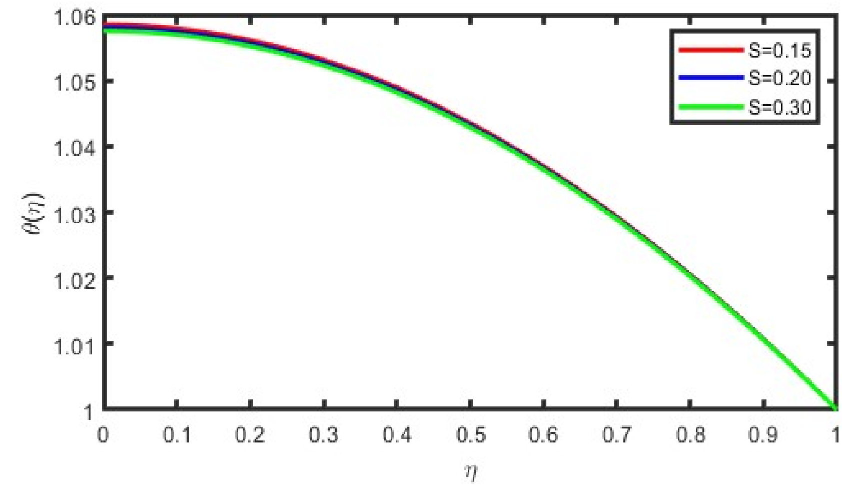

FIGURE 9 IMPACT OF B ON Θ(H)

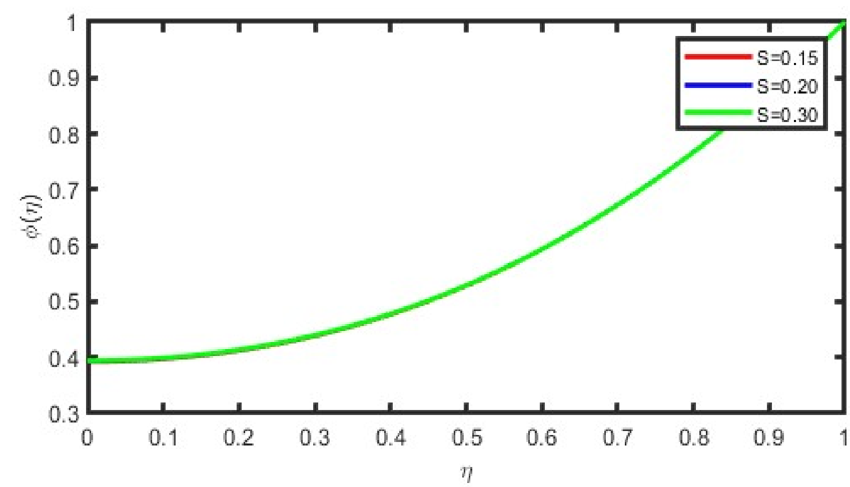

FIGURE 10 IMPACT OF B ON ϕ (H)

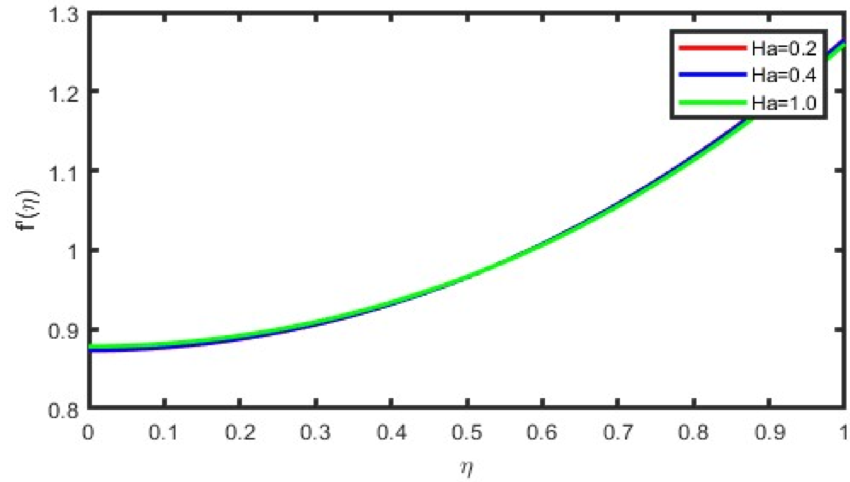

FIGURE 11 IMPACT OF HA ON F(H)

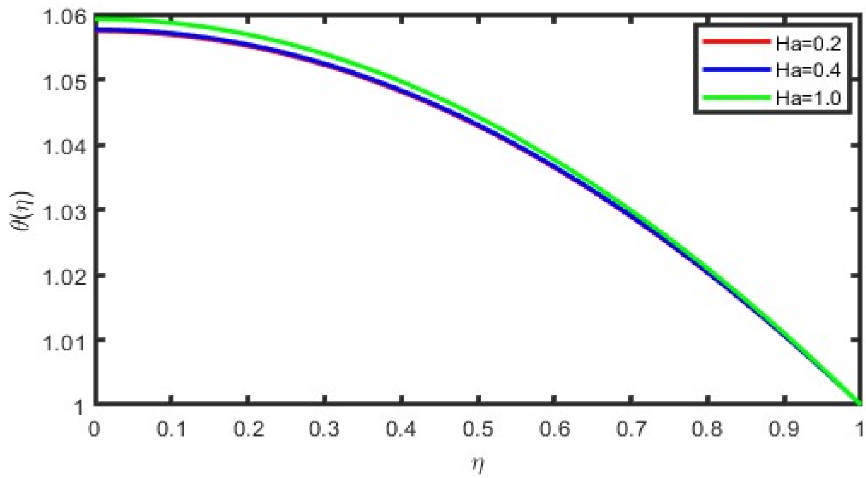

FIGURE 12 IMPACT OF HA ON Θ(H)

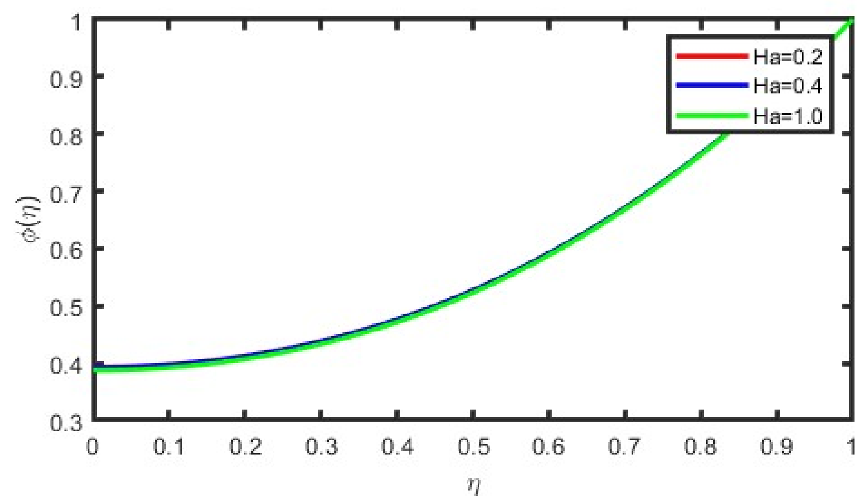

FIGURE 13 IMPACT OF HA ON ϕ (H)

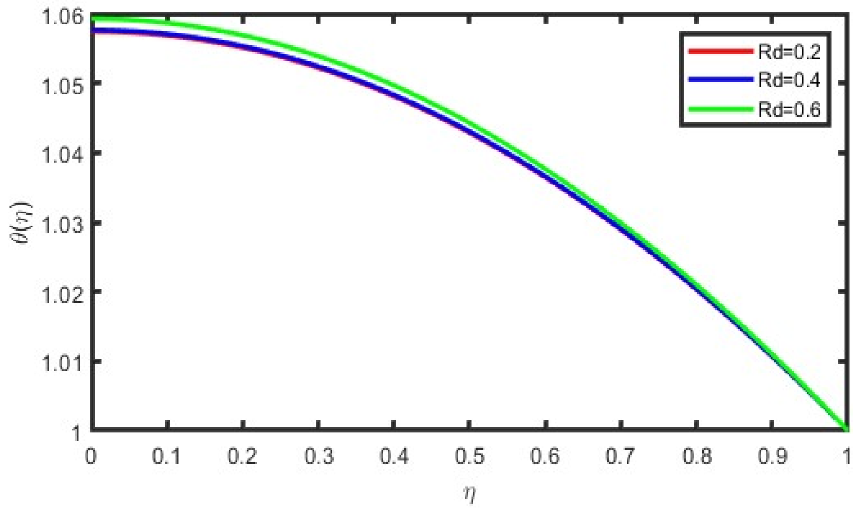

FIGURE 14 IMPACT OF RD ON Θ(H)

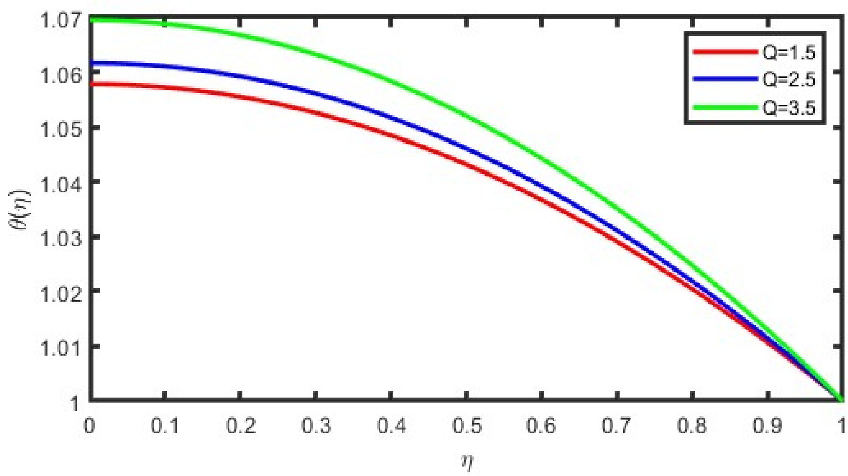

FIGURE 15 IMPACT OF Q ON Θ(H)

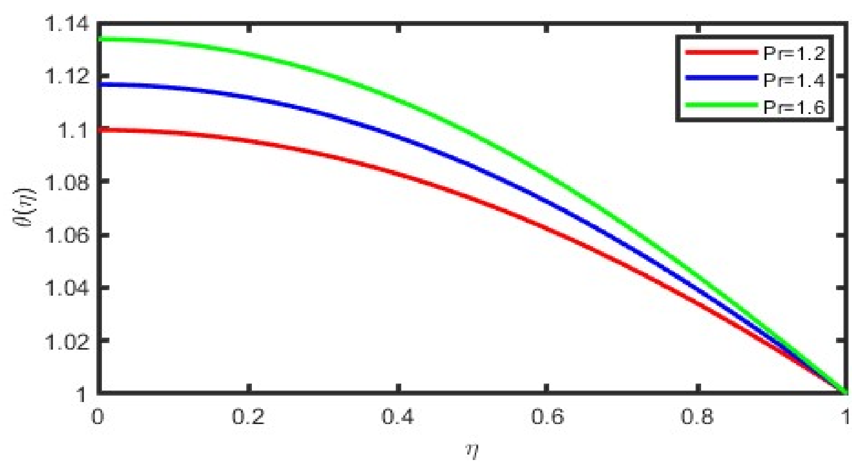

FIGURE 16 IMPACT OF PR ON Θ(H)

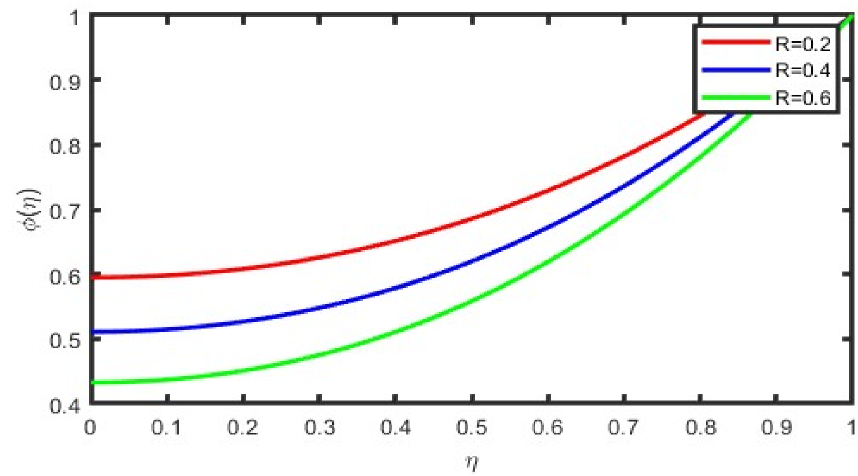

FIGURE 17 IMPACT OF R ON ϕ (H)

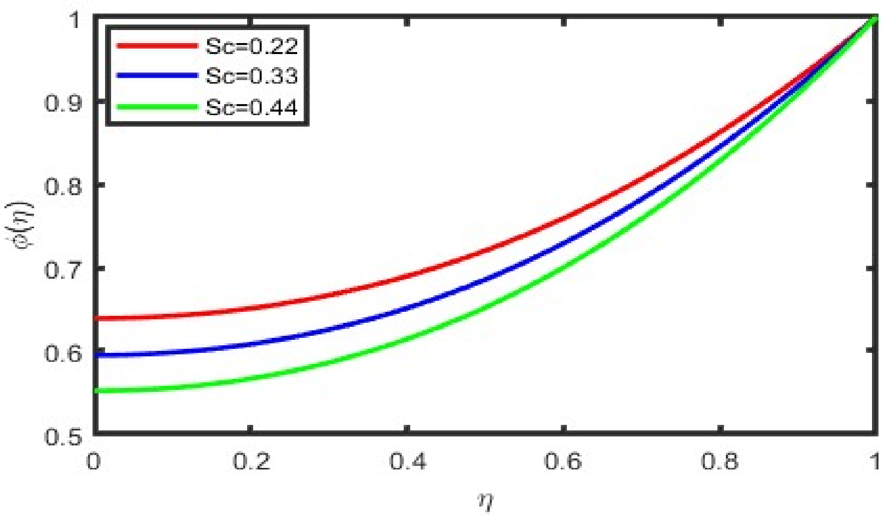

FIGURE 18 IMPACT OF SC ON ϕ (H)

6 CONCLUSIONS

1. The heat and mass transfer characteristics of unsteady MHD flow of Casson nanofluid squeezing between two parallel plates saturated in a porous medium under the influence of chemical reaction, thermal radiation and heat generation or absorption was investigated numerically. The effects of viscous and Joule dissipation were also considered. The flow is induced by the motion of the upper plate towards or away from lower plate with an external velocity. The use of the Shooting technique derives the numerical answers. The numerical solutions for skin friction coefficient, Nusselt and Sherwood numbers are validated with the previous works and excellent agreement is observed from both results. The effects of physical parameters, namely, squeeze number S, Casson fluid parameter β, Hartmann number Ha, radiation parameter Rd, heat generation/absorption parameter Q and chemical reaction parameter R on fluid velocity, temperature and concentration are analysed graphically. The main findings of this study can be summarized as follows.

2. In view of industrial use, the power required to generate the movement of the parallel plates is considerably reduced for the negative values of squeezing number. The influence of negative and positive squeezing parameter on velocity field is observed to be reversed. The higher values of squeezing number diminish the squeezing force on the fluid flow, which in turn reduces the thermal field. The thinner temperature boundary layer corresponds to the lower values of thermal diffusivity and it shows the higher values of temperature gradient for the increasing values of β. Due to the presence of stronger Lorentz forces the temperature and velocity fields behave like decreasing functions of Hartmann number. Temperature field is suppressed for the increasing values of thermal radiation parameter. The destructive chemical reaction intensifies the concentration field and constructive chemical reaction decreases the concentration field. The current numerical investigation has provided some remarkable insights of squeezing flow with non-Newtonian Casson fluid between two parallel plates. The numerical results presented in this paper may be useful in theoretical and experimental studies related to the squeezing flow phenomena.

3. References

4. J. Stefan, "Versucheuber die scheinbare adh ¨ asion," ¨ Akadenie deer Wissenschaften in Wien, Math.-Naturw, vol. 69, pp. 713– 721, 1874.
5. QD. F. Moore, "A review of squeeze films," Wear, vol. 8, no. 4, pp. 245–263, 1965.
6. P. S. Gupta and A. S. Gupta, "Squeezing flow between parallel plates," Wear, vol. 45, no. 2, pp. 177–185, 1977.
7. H. M. Duwairi, B. Tashtoush, and R. A. Damseh, "On heat transfer effects of a viscous fluid squeezed and extruded between two parallel plates," Heat and Mass Transfer, vol. 41, no. 2, pp. 112–117, 2004.
8. R. L. Verma, "A numerical solution for squeezing flow between parallel channels," Wear, vol. 72, no. 1, pp. 89–95, 1981.
9. M. Mustafa, T. Hayat, and S. Obaidat, "On heat and mass transfer in the unsteady squeezing flow between parallel plates," Meccanica, vol. 47, no. 7, pp. 1581–1589, 2012.
10. T. Hayat, A. Qayyum, F. Alsaadi, M. Awais, and A. M. Dobaie, "Thermal radiation effects in squeezing flow of a Jeffery fluid," European Physical Journal Plus, vol. 128, no. 8, pp. 85–91, 2013.
11. E. W. Mrill, A. M. Benis, E. R. Gilliland, T. K. Sherwood, and E. W. Salzman, "Pressure-flow relations of human blood in hollow fibers at low flow rates," Journal of Applied Physiology, vol. 20, no. 5, pp. 954–967, 1965.
12. D. A. McDonald, Blood Flows in Arteries, Arnold, London, UK, 2nd edition, 1974.
13. H. I. Andersson and B. S. Dandapat, "Flow of a powerlaw fluid over a stretching sheet," Applied Analysis of Continuous Media, vol. 1, no. 339, 1992.
14. M. Sajid, I. Ahmad, T. Hayat, and M. Ayub, "Unsteady flow and heat transfer of a second grade fluid over a stretching sheet," Communications in Nonlinear Science and Numerical Simulation, vol. 14, no. 1, pp. 96–108, 2009.

15. N. Casson, Rheology of Dispersed System, vol. 84, Pergamon Press, Oxford, UK, 1959.

16. R. K. Dash, K. N. Mehta, and G. Jayaraman, "Casson fluid flow in a pipe filled with a homogeneous porous medium," International Journal of Engineering Science, vol. 34, no. 10, pp. 1145–1156, 1996.

17. N. T. M. Eldabe and M. G. E. Salwa, "Heat transfer of mhd non-newtonian casson fluid flow between two rotating cylinder," Journal of the Physical Society of Japan, vol. 64, p. 4164, 1995.

18. M. H. Hamdan, "An alternative approach to exact solutions of a special class of Navier-Stokes flows," Applied Mathematics and Computation, vol. 93, no. 1, pp. 83–90, 1998.

19. Hamdan and F. M. Allan, "A note on the generalized Beltrami flow through porous media," International Journal of Pure and Applied Mathematics, vol. 27, no. 4, pp. 491–500, 2006.

20. K. Vafai and C. L. Tien, "Boundary and inertia effects on flow and heat transfer in porous media," International Journal of Heat and Mass Transfer, vol. 24, no. 2, pp. 195–203, 1981.

21. S. Islam, M. R. Mohyuddin, and C. Y. Zhou, "Few exact solutions of non-Newtonian fluid in porous medium with hall effect," Journal of Porous Media, vol. 11, no. 7, pp. 669–680, 2008.

22. K. Vafai, Handbook of Porous Media, CRC Press, Taylor and Francis, Boca Raton, Fla, USA, 2nd edition, 2005.

23. P. Durga Prasad, V. M. S. S. K. Kumar, and S. V. K. Varma, S, Heat and mass transfer analysis for the MHD flow of nanofluid with radiation absorption, Ain Shams Engineering Journal, 9, 801-813 (2018). 10.1016/j.asej.2016.04.016.

24. S. P. Samrat, C. Sulochana, G. P. Ashwinkumar, Impact of Thermal Radiation on an Unsteady Casson Nanofluid Flow over a Stretching Surface, Int. J. Appl. Comput. Math (2019) 5:31 https://doi.org/10.1007/s40819-019-0606-2

25. K. Raghunath, G. Nagesh, V. R. C. Reddy, M. Obulesu, Unsteady MHD fluid flow past an inclined vertical porous plate in the presence of chemical reaction with aligned magnetic field, radiation, and Soret effects, Heat Transfer, Vol 51, 1-19 (2021). DOI: 10.1002/htj.22423.

26. Raghunath Kodi, Obulesu Mopuri, Unsteady MHD oscillatory Casson fluid flow past an inclined vertical porous plate in the presence of chemical reaction with heat absorption and Soret effects, Heat Transfer, Vol 51 (3), 1-19 (2021). DOI: 10.1002/htj.22327

27. Raghunath Kodi, Obulesu Mopuri, Sujatha Sree, Venkateswaraju Konduru, Investigation of MHD Casson fluid flow past a vertical porous plate under the influence of thermal diffusion and chemical reaction, Heat Transfer, Vol 51 (3), 77–394 (2021). DOI: 10.1002/htj.22311

28. Ramachandra Reddy Vaddemani, Raghunath Kodi , Obulesu Mopuri, Characteristics of MHD Casson fluid past an inclined vertical porous plate, Materials Today: Proceedings , Vol 49, 2136–2142 (2022). https://doi.org/10.1016/j.matpr.2021.08.328.

29. C. Sulochana, G.P. Ashwinkumar, N. Sandeep, Effect of frictional heating on mixed convection flow of chemically reacting radiative Casson nanofluid over an inclined porous plate, Alexandria Engineering Journal, Volume 57, Issue 4, 2018, Pages 2573-2584, https://doi.org/10.1016/j.aej.2017.08.006.
30. K.J. Rani, Ch.V.R. Murthy, Radiation absorption on an unsteady convective heat and mass transfer flow past a semi-infinite inclined permeable plate embedded in a porous medium, Int. J. Eng. Sci. Technol., 4 (3) (2012), pp. 1052-1065.
31. Ullah, Imran, Krishnendu Bhattacharyya, Sharidan Shafie, and Ilyas Khan. "Unsteady MHD mixed convection slip flow of Casson fluid over nonlinearly stretching sheet embedded in a porous medium with chemical reaction, thermal radiation, heat generation/absorption and convective boundary conditions." PLoS ONE 11, no. 10 (2016): e0165348. https://doi.org/10.1371/journal.pone.0165348
32. ong, Jian, Weijian An, Yingwei Wu, and Wenxi Tian. "Neutronics and thermal hydraulics analysis of a conceptual ultra-high temperature MHD cermet fuel core for nuclear electric propulsion." Frontiers in Energy Research 6, no. 29 (2018). https://doi.org/10.3389/fenrg.2018.00029
33. Saadati, Hassan, Kamal Hadad, and Ataollah Rabiee. "Safety margin and fuel cycle period enhancements of VVER1000 nuclear reactor using water/silver nanofluid." Nuclear Engineering and Technology 50, no. 5 (2018): 639-647. https://doi.org/10.1016/j.net.2018.01.015
34. Shankar, Usha, and Neminath Bujjappa Naduvinamani. "Magnetized impacts of Brownian motion and thermophoresis on unsteady squeezing flow of nanofluid between two parallel plates with chemical reaction and Joule heating." Heat Transfer-Asian Research 48, no. 8 (2019): 4174-4202. https://doi.org/10.1002/htj.21587
35. Noor, Nur Azlina Mat, Sharidan Shafie, and Mohd Ariff Admon. "Effects of viscous dissipation and chemical reaction on MHD squeezing flow of Casson nanofluid between parallel plates in a porous medium with slip boundary condition." The European Physical Journal Plus 135, no. 10 (2020): 1-24. https://doi.org/10.1140/epjp/s13360-020- 00868-w
36. I.C. Mandal, S. Mukhopadhyay, Nonlinear convection in micropolar fluid flow past an exponentially stretching sheet in an exponentially moving stream with thermal radiation, Mech. Adv. Mater. Struct. 26 (24) (2019) 2040e2046.
37. K.A. Kumar, V. Sugunamma, N. Sandeep, Effect of thermal radiation on MHD Casson fluid flow over an exponentially stretching curved sheet, J. Therm. Anal. Calorim. 140 (5) (2020) 2377e2385.
38. S.S. Ghadikolaei, M. Gholinia, M.E. Hoseini, D.D. Ganji, Natural convection MHD flow due to MoS2-Ag nanoparticles suspended in C2H6O2-H2O hybrid base fluid with thermal radiation, Journal of the Taiwan Institute of Chemical Engineers 97 (2019) 12e23.
39. Z. Asghar, K. Javid, M. Waqas, A. Ghaffari, W.A. Khan, Cilia-driven fluid flow in a curved channel: effects of complex wave and porous medium, Fluid Dynam. Res. 52 (1) (2020) 015514.

40. K. Ramesh, Influence of heat and mass transfer on peristaltic flow of a couple stress fluid through porous medium in the presence of inclined magnetic field in an inclined asymmetric channel, J. Mol. Liq. 219 (2016) 256e271.
41. N.S. Akbar, A.W. Butt, D. Tripathi, O.A. Bég, Physical hydrodynamic propulsion model study on creeping viscous flow through a ciliated porous tube, Pramana 88 (3) (2017) 52.
42. K. Ramesh, S.A. Eytoo, Effects of thermal radiation and magnetohydrodynamics on ReeEyring fluid flows through porous medium with slip boundary conditions, Multidiscip. Model. Mater. Struct. 15 (2) (2019) 492e507.
43. K. Ramesh, D. Kumar, M. Devakar, Electrokinetically modulated flow of couple stress magnetonanofluids in a microfluidic channel, Heat Tran. Asian Res. 48 (1) (2019) 379e397.
44. R. K. Dash, KN. Mehta, G. Jayaraman, Casson fluid flow in a pipe filled with homogeneous porous medium, International journal of engineering Science, 34(1996), 1145-1156.
45. Ahmed N, Khan U, Khan S I, Bano S and Mohyud-Din S T 2017 Effects on magnetic field in squeezing flow of a Casson fluid between parallel plates. J. King Saud Univ. Sci. 29: 119–125
46. Mohyud-Din, Syed Tauseef, Muhammad Usman, Wei Wang, and Muhammad Hamid. "A study of heat transfer analysis for squeezing flow of a Casson fluid via differential transform method." Neural Computing and Applications 30, no. 10 (2018): 3253-3264. https://doi.org/10.1007/s00521-017-2915-x
47. Nur Azlina Mat Noor, Mohd Ariff Admon, Sharidan Shafie, Unsteady MHD Squeezing Flow of Casson Fluid Over Horizontal Channel in Presence of Chemical Reaction, Journal of Advanced Research in Fluid Mechanics and Thermal Sciences 92, Issue 2 (2022) 49-60.
48. Pourmehran, O., M. Rahimi-Gorji, M. Gorji-Bandpy, and D. D. Ganji. "Analytical investigation of squeezing unsteady nanofluid flow between parallel plates by LSM and CM." Alexandria Engineering Journal 54 (2015): 17-26. https://doi.org/10.1016/j.aej.2014.11.002
49. Noor, Nur Azlina Mat, Sharidan Shafie, and Mohd Ariff Admon. "MHD squeezing flow of casson nanofluid with chemical reaction, thermal radiation and heat Generation/Absorption." Journal of Advanced Research in Fluid Mechanics and Thermal Sciences 68, no. 2 (2020): 94-111. https://doi.org/10.37934/arfmts.68.2.94111
50. N. B. Naduvinamani, Usha Shankar, Radiative squeezing flow of unsteady magneto-hydrodynamic Casson fluid between two parallel plates, J. Cent. South Univ. (2019) 26: 1184−1204 DOI: https://doi.org/10.1007/s11771-019-4080-0.
51. Cebeci T, Bradshaw P. Physical and computational aspects of convective heat transfer [M]. USA: SpringerVerlag, 1984.